Ther Adv Gastroenterol
2019, Vol. 12: 1–14
DOI: 10.1177/1756284819827697

Long noncoding RNA *AOC4P* regulates tumor cell proliferation and invasion by epithelial–mesenchymal transition in gastric cancer

Kecheng Zhang, Canrong Lu, Xiaohui Huang, Jianxin Cui, Jiyang Li, Yunhe Gao, Wenquan Liang, Yi Liu, Yang Sun, Hanxuan Liu, Bo Wei and Lin Chen

Abstract

Background: The clinical relevance and biological role of tissular *AOC4P* in gastric cancer (GC) remains to be clarified.

Methods: The association between *AOC4P* expression and clinicopathological characteristics was investigated. *In vitro*, 3-(4,5-dimethylthiazol-2-yl)-2,5-diphenyltetrazolium bromide (MTT), colony formation, wound healing and terminal deoxynucleotidyl transferase dUTP nick end labeling (TUNEL) assays were performed to explore the biological effects of *AOC4P* on GC cell proliferation, migration, invasion, and apoptosis in MGC-803 and BGC-823 cell lines. *In vivo*, animal experiments were conducted to confirm the *in vitro* findings. Quantitative real-time polymerase chain reaction, western blotting, and immunofluorescence were used to investigate the potential mechanisms.

Results: Expression levels of *AOC4P* were significantly higher in tumor tissues than in noncancerous tissues, and patients with high levels of *AOC4P* had poor overall and disease-free survival. *AOC4P* expression was correlated with lymphovascular invasion. *In vitro*, knockdown of *AOC4P* inhibited tumor cell proliferation, migration, and invasion, and promoted apoptosis of MGC-803 and BGC-823 cells. *In vivo*, BGC-823 cells transfected with *AOC4P* siRNA formed smaller and lighter tumors than BGC-823 cells transfected with negative control siRNA in severe combined immunodeficiency mice. Additionally, the si-*AOC4P* group had less proliferating cells and more apoptotic cells in tumor xenografts compared with the negative control. Mechanistically, knockdown of *AOC4P* decreased the expression of vimentin and MMP9, while increasing the expression of E-cadherin. Immunofluorescence confirmed the relationship between *AOC4P* expression and E-cadherin, vimentin, and MMP9 levels in clinical GC specimens.

Conclusions: *AOC4P* promotes tumorigenesis and progression partly through epithelial–mesenchymal transition in GC. Additionally, *AOC4P* may serve as a prognostic biomarker for clinical decision making.

Keywords: *AOC4P*, long noncoding RNAs, metastasis, prognosis, stomach neoplasm

Received: 2 July 2018; revised manuscript accepted: 19 December 2018.

Correspondence to:
Lin Chen
Department of General Surgery & Institute of General Surgery, Chinese People's Liberation Army General Hospital, Fuxing Road 28, Beijing 100853, PR China
chenlin@301hospital.com.cn

Kecheng Zhang
Canrong Lu
Xiaohui Huang
Jianxin Cui
Jiyang Li
Yunhe Gao
Wenquan Liang
Yi Liu
Bo Wei
Department of General Surgery & Institute of General Surgery, Chinese People's Liberation Army General Hospital, Beijing, PR China

Yang Sun
Department of Ultrasound, Peking University Third Hospital, Beijing, PR China

Hanxuan Liu
Medical Experiment and Analysis Center, Chinese People's Liberation Army General Hospital, Beijing, PR China

Background

Gastric cancer (GC) is a heterogeneous disease with an estimated 5-year overall survival of 27.4% in China.[1] Current approaches for GC management largely depend on multimodal therapeutic strategies including gastrectomy, chemotherapy, and chemoradiotherapy in perioperative settings. However, 25–40% of GC patients have recurrence after treatment.[2–4] Hence, more research that focuses on the molecular mechanisms promoting cancer progression is needed, which would aid in the discovery and development of

effective diagnostic biomarkers and therapeutic targets for GC and thus provide patients with potentially better outcomes.[5,6]

Long noncoding RNA (lncRNA) is a class of RNAs of 200 nucleotides in length without a protein-coding ability. Sequencing technologies have shown that only <2% of transcripts transcribed from the human genome code for proteins,[7,8] leaving much of the noncoding transcripts unexplored. Recent studies have revealed that lncRNAs are associated with GC tumorigenesis and metastasis, and have the potential to serve as diagnostic and prognostic biomarkers.[9,10] For example, our previous study established a novel five plasma lncRNA-based panel [terminal differentiation-induced noncoding RNA (*TINCR*), *CCAT2, AOC4P*, BRAF-activated noncoding RNA (*BANCR*) and *LINC00857*] that discriminates GC from precancerous individuals with relatively high accuracy compared with widely used serum carcinoembryonic antigen, CA19-9, and CA125.[11] However, the molecular mechanism of these lncRNAs in GC initiation and development need to be clarified further.

In the present study, we investigated the clinical relevance and biological role of *AOC4P* in GC, as the role of *TINCR, CCAT2, BANCR* and *LINC00857* in GC has been previously reported.

Methods

Tissue specimens

GC tissues and adjacent normal tissues were collected from 63 patients who underwent surgery between January 2013 and December 2013 at the Department of General Surgery, Chinese PLA General Hospital. All patients were diagnosed by pathology. None of the patients had received preoperative chemotherapy or radiochemotherapy. Patient characteristics were obtained, including age, sex, T stage, lymph node status, tumor size, tumor differentiation, and TNM (tumor-node-metastasis) stage according to the 7th edition American Joint Committee on Cancer Staging manual. Patients were followed up every 6 months. Patients with suspicion of recurrence were assessed by computed tomography. The last follow-up time was May 2017. Disease-free survival and overall survival times were calculated. All patients provided written informed consent about their tumor specimen for research use. The collection and use of patient's specimen was approved by the Ethics Committee of the Chinese PLA General Hospital (NO.S2016-057-01).

Cell lines and culture

Human GC cell lines MGC-803 and BGC-823 were purchased from the Chinese Academy of Sciences Committee on Type Culture Collection cell bank (Shanghai, China). The immortalized human gastric epithelial cell line GES-1 was obtained from the Institute of General Surgery at the Chinese PLA General Hospital. The cell lines were cultured as described previously.[11]

RNA extraction and quantitative real-time polymerase chain reaction

RNA was extracted from tissues and cultured cells using Trizol reagent (Invitrogen, Carlsbad, CA, USA), according to the manufacturer's protocol. RNA concentrations and purity were measured by a NanoDrop 2000/2000c spectrophotometer (Thermo Fisher Scientific, Wilmington, USA). cDNA was synthesized from 3 μg extracted RNA using a reverse transcription kit (Invitrogen). Quantitative real-time polymerase chain reaction (qRT-PCR) was performed as described previously.[11] Primer sequences are shown in the supplementary files.

Western blot assay

Western blot assays were performed as described previously.[12] In brief, extracted proteins from tissues and cell lines were separated by sodium dodecyl sulfate polyacrylamide gel electrophoresis and then transferred to polyvinylidene fluoride membranes (Bio-Rad Laboratories, USA). After blocking, the membranes were incubated with a primary antibody overnight at 4°C. Then, the blotted membranes were incubated with a horseradish peroxidase-conjugated secondary antibody (1:2000) for 2 h at room temperature. Labeled proteins were detected using enhanced chemiluminescence following the manufacturer's protocol. β-Actin (1:1000, Cell Signaling, USA) was used as an internal control. Antibodies against the following proteins were used: E-cadherin (1:1000, Cell Signaling), matrix metalloproteinase-9 (MMP-9; 1:1000, Abcam, USA), vimentin (1:1000, Cell Signaling), cleaved caspase-3 (1:1000, Cell Signaling) and

cleaved poly (ADP-ribose) polymerase (PARP; 1:1000, Cell Signaling).

Immunohistochemistry

Immunohistochemistry (IHC) was performed using a standard technique with an avidin-biotinylated peroxidase complex as described previously.[12,13] Sections were incubated with an anti-Ki-67 antibody (1:400, Cell Signaling) at 4°C overnight. Diaminobenzidine (DAKO, China) staining was used to detect immunoreactivity. The intensity of immunoreactivity was graded as 0, 1+, 2+, and 3+ for no staining, weak, medium, and strong staining, respectively. Scores of 0 and 1+ were regarded as low expression, while scores of 2+ and 3+ were considered as high expression. The proliferation index of the cancer cells = high expression cells/total cells × 100%.

Immunofluorescence staining

The 5 μm-thick, formalin-fixed, paraffin-embedded tissue sections were incubated with a primary antibody at 4°C overnight. Then, the sections were rinsed three times for 5 min each with phosphate-buffered saline (PBS) followed by incubation with Alexa Fluor-conjugated secondary antibodies at room temperature for 1 h. Fluorescence imaging was performed using a laser scanning confocal microscope (Fluoview FV1000, Olympus, Japan). Fluorescence staining was quantified using Tissue-Quest software (TissueGnostics GmbH). Tumor tissues were classified as high or low expression using a cutoff of the mean expression level of proteins (high expression ⩾ mean; low expression < mean). Antibodies against the following proteins were used: E-cadherin (1:100, Cell Signaling), MMP-9 (1:500, Abcam), and vimentin (1:100, Cell Signaling).

Colony formation assay

A total of 500 cells per well were seeded in a six-well plate in triplicate and maintained in a humidified atmosphere containing 5% CO_2 at 37°C. After culture for 10–14 days, cell colonies were washed with PBS, fixed with 4% paraformaldehyde for 30 min, and stained with a 0.1% crystal violet solution for 20 min. Colonies containing more than 50 cells were counted.

Proliferation assay

Proliferation of cells was measured by MTT assays using Cell Proliferation Reagent Kit I (Roche Applied Science, USA), according to the manufacturer's protocols. A total of 3×10^3 cells/well transfected with the indicated vector were seeded in a 96-well flat-bottomed plate and cultured in normal medium for 24 h. At 0, 24, 48, 72 and 96 h after transfection, MTT solution (5 mg/ml, 20 μl) was added to each well. The relative number of surviving cells was assessed by measuring the optical density of cell lysates at 560 nm. For each treatment group, cells were assessed in triplicate.

Cell migration and invasion assays

Cell migration was measured using a Transwell chamber with an 8 μm pore size membrane according to the manufacturer's instructions. In brief, 3×10^5 cells in 200 μl serum-free medium were added to the upper chamber. For the invasion assay, 5×10^5 cells in 200 μl serum-free medium were added to the upper chamber coated with 1 mg/ml Matrigel. Subsequently, 500 μl serum-containing medium was added to the lower chamber. Cells were incubated at 37°C for 24 h, and then cells on the upper surface of the membrane were scraped off with cotton swabs. Cells that had migrated and invaded to the lower surface of the membrane were fixed and stained with a 0.1% crystal violet solution. Four random microscopic fields of the membrane were photographed, and cells were counted for statistical analysis.

Wound healing assay

A total of 5×10^5 cells per well were seeded in six-well plates and cultured until 90% confluence. A 200 μl sterile pipette tip was used to make a straight scratch on the culture surface. Detached cells were washed off gently, and images of the scratch were photographed as a baseline. The medium was then replaced, and images of the same location were obtained under a microscope after 48 h. The healing rate was calculated as follows: $(\text{Width}_{\text{baseline}} - \text{Width}_{48h})/\text{Width}_{\text{baseline}}$.

Flow cytometric analysis

Cells were harvested, washed with PBS and fixed overnight in 4% formaldehyde at −20°C. Then, the cell was stained with propidium iodide using

cell cycle kit (BD Biosciences, NJ, USA) according to the manufacturer's instructions. The cells were analyzed by FACScan (BD Biosicences, Franklin Lakes, NJ, USA).

In vivo *tumorigenicity*

Animal experiments were conducted in accordance with the recommendations in the Guide for the Care and Use of Laboratory Animals of the National Institutes of Health. Animal experiments were approved by the Animal Care and Use Committee of Chinese PLA Hospital. The 4-week-old severe combined immunodeficiency mice were maintained under specific pathogen-free conditions. BGC-823 cells stably transfected with *AOC4P* siRNA (si-*AOC4P*) or the empty vector were harvested and washed. Then, 5×10^6 cells transfected with si-*AOC4P* or the empty vector were injected subcutaneously into the left and right flanks of each mouse, respectively. Tumor volumes were measured by ultrasound every 7 days, and the mice were euthanized after 4 weeks. Tumor volumes were calculated by the following formula[14]: (width^2 × length)/2.

Terminal deoxynucleotidyl transferase dUTP nick end labeling assay

Tumor xenografts were fixed in 4% formalin and embedded in paraffin. An *in situ* terminal deoxynucleotidyl transferase dUTP nick end labeling (TUNEL) kit (Roche Applied Science) was used to detect cell apoptosis in the implanted tumors according to the manufacturer's protocol. Apoptotic cells and the total number of cells in five random fields were counted in each group. The apoptotic index of the cancer cells = apoptotic cells/total cells × 100%.

Statistical analysis

Data are expressed as the mean ± standard deviation (SD) and were analyzed with SPSS software version 22.0. Continuous variables were analyzed using an independent Student's *t*-test or paired *t*-test. Discrete variables were compared using the Chi-square test or Fisher's exact test. Kaplan–Meier plots were used to analyze overall and disease-free survival that was compared by the log-rank test. Univariate and multivariate Cox regression analysis was performed to investigate the prognostic factors. A two-sided *p* value of less than 0.05 was considered as statistically significant.

Results

AOC4P *is upregulated in GC cell lines and tumor tissues*

To investigate the expression levels of *AOC4P* in GC, we performed qRT-PCR in two GC cell lines (MGC-803 and BGC-823) and a human gastric epithelial cell line (GES-1). Consistent with our previous study, as shown in Figure 1(a), *AOC4P* was highly expressed in GC cell lines compared with the gastric epithelial cell line. Next, we determined the relative expression of *AOC4P* in 63 paired GC tumor tissues and corresponding adjacent noncancerous tissues. The expression levels of *AOC4P* were also significantly higher in tumor tissues than in noncancerous tissues, suggesting involvement of *AOC4P* in the tumorigenesis of GC [Figure 1(b)].

High expression of AOC4P *correlates with poor prognoses*

Using the median expression level of *AOC4P* in tumor tissues as the cutoff, we divided the patients into two groups: patients with high or low expression of *AOC4P* [Figure 1(c)]. After a median follow-up time of 41 months (range: 4–49 months), as illustrated in Figure 1(d), patients with a high expression level of *AOC4P* had poorer overall survival than those with a low expression level of *AOC4P*. Similarly, patients with high expression of *AOC4P* had poorer disease-free survival [Figure 1(e)]. Additionally, expression of *AOC4P* was correlated with lymphovascular invasion (Table 1), a critical step for tumor dissemination. As shown in Table 2, univariate and multivariate Cox regression analysis has revealed that *AOC4P* expression was strongly associated with disease-free survival and overall survival. These findings suggest that *AOC4P* is associated with metastasis and can serve as a prognostic biomarker.

Knockdown of AOC4P *inhibits cellular proliferation and colony formation in vitro*

To investigate the biological effects of *AOC4P* on cellular growth and colony formation, loss-of-function experiments were conducted. We first knocked down *AOC4P* expression by transfection of si-*AOC4P* into MGC-803 and BGC-823 cells. The results of qRT-PCR analyses revealed that *AOC4P* expression was knocked

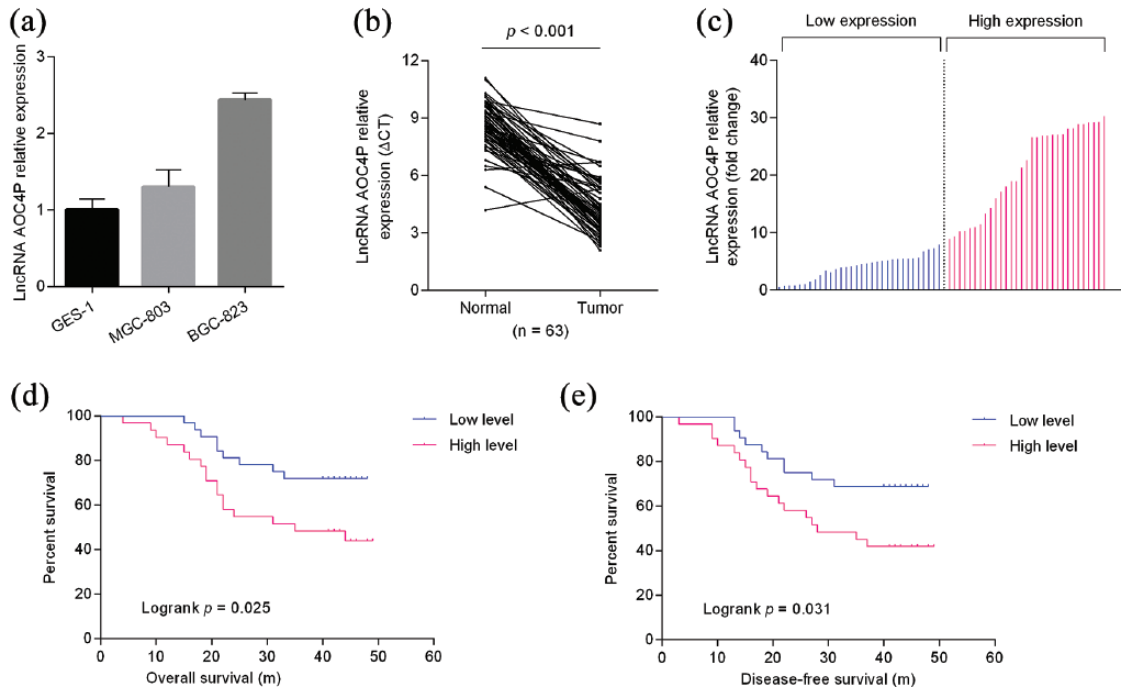

Figure 1. *AOC4P* expression levels in GC cell lines and specimens, and its prognostic value for GC. (a) Determination of *AOC4P* expression in GES-1, MGC-803 and BGC-823 cells by qRT-PCR. (b) Determination of *AOC4P* expression in GC specimens. (c) Relative expression of *AOC4P* in tumor tissues. (d) Correlation of *AOC4P* expression with overall survival. (e) Correlation of *AOC4P* expression with disease-free survival.
GC, gastric cancer; qRT-PCR, quantitative real-time polymerase chain reaction.

down by 89% and 83% in si-*AOC4P*-transfected MGC-803 and BGC-823 cells, respectively, compared with siRNA negative control (si-NC)-transfected cells (Figure S1). MTT assays showed inhibition of cell growth by knockdown of *AOC4P* expression in MGC-803 and BGC-823 cells compared with controls [Figure 2(a)]. Additionally, clonogenic abilities were impaired following downregulation of *AOC4P* in MGC-803 and BGC-823 cells [Figure 2(b)]. *In situ* TUNEL assays revealed that the proportion of apoptotic cells was higher among si-*AOC4P*-transfected MGC-803 and BGC-823 cells than si-NC-transfected cells [Figure 2(c)]. Flow cytometric analysis revealed that knockdown of *AOC4P* significantly increased GC cells in the G0/G1 phase, while reduced cells in the S phase [Figure 3(a)]. Meanwhile, western blot assay showed that the expression of apoptosis-related proteins, including cleaved caspase-3 and cleaved PARP, were significantly increased after knockdown of *AOC4P* [Figure 3(b)]. Collectively, these data indicate that knockdown of *AOC4P* inhibits GC cells proliferation and promotes apoptosis.

Effect of AOC4P *on migration and invasion of GC cells*

We used Transwell and wound healing assays to determine the effect of *AOC4P* on migration and invasion of GC cells. As shown in Figure 4(a) and (b), the migration and invasion abilities of GC cells were significantly decreased when *AOC4P* expression was reduced in MGC-803 and BGC-823 cells. These results suggested that *AOC4P* promotes the migration and invasion of GC cells.

Knockdown of AOC4P *inhibits GC tumorigenesis* in vivo

To explore whether *AOC4P* affects tumorigenesis *in vivo*, BGC-823 cells were stably transfected with si-*AOC4P* or the empty vector and then injected subcutaneously into the left and right flanks of each mouse, respectively. At 14 days after injection, tumors formed in the si-*AOC4P* group were significantly smaller than those in the si-NC group [Figure 5(a) and (b)]. The tumor weight was also lower in the si-*AOC4P* group compared with the si-NC group [Figure 5(c)]. qRT-PCR analysis revealed that *AOC4P* expression was significantly

Table 1. Relationship between expression level of *AOC4P* and characteristics.

Characteristics	No.	lncRNA *AOC4P* expression		*p* value
		Low expression ($n = 31$)	High expression ($n = 32$)	
Age, years				0.373
>60	21	12	9	
⩽60	42	19	23	
Sex				0.353
Female	17	10	7	
Male	46	21	25	
pT stage				0.252
T1/T2	14	5	9	
T3/T4	49	26	23	
Lymph node				0.822
Positive	15	7	8	
Negative	48	24	24	
Lymphovascular invasion				**0.0021**
Positive	22	5	17	
Negative	41	26	15	
Perineural invasion				0.353
Positive	17	10	7	
Negative	46	21	25	
pTNM stage				0.163
I	7	3	4	
II	29	11	18	
III	27	17	10	

lncRNA, long noncoding RNA; TNM, tumor, nodes, metastasis.

lower in si-*AOC4P* tumor xenografts [Figure 5(d)]. The results of IHC and *in situ* TUNEL assays of xenografts showed that si-*AOC4P* tumor xenografts had reduced proportions of Ki-67-positive cells and increased proportions of TUNEL-positive cells compared with si-NC tumor xenografts [Figure 4(e)]. Consistent with the aforementioned *in vitro* results, these data indicate that *AOC4P* affects GC tumorigenesis *in vivo*.

AOC4P *modulates GC tumorigenesis* via *epithelial–mesenchymal transition*

A recent study reported that *AOC4P* suppresses hepatocellular carcinoma *via* inhibition of epithelial–mesenchymal transition (EMT).[15] Therefore, we investigated whether *AOC4P* functions in a similar manner in GC. After knockdown of *AOC4P* in BGC-823 and MGC-803 cells, qRT-PCR analysis revealed an increase in E-cadherin

Table 2. Univariate and multivariate Cox regression analysis for DFS and OS.

Variables	DFS		OS	
	HR (95% CI)	*p* value	HR (95% CI)	*p* value
Univariate analysis				
Age (>60 *versus* ⩽60 years)	1.43 (0.67–3.06)	0.354	1.72 (0.79–3.74)	0.174
Sex (female *versus* male)	1.83 (0.84–3.98)	0.128	1.46 (0.98–2.18)	0.061
pT stage (T3/T4 *versus* T1/T2)	1.06 (0.43–2.61)	0.906	0.96 (0.39–2.40)	0.937
Lymph node (positive *versus* negative)	4.78 (2.22–10.27)	<0.001	4.91 (2.23–10.79)	<0.001
Lymphovascular invasion (positive *versus* negative)	3.49 (1.64–7.43)	0.001	4.12 (1.86–9.130)	<0.001
Perineural invasion (positive *versus* negative)	1.59 (0.75–3.34)	0.223	1.34 (0.62–2.90)	0.452
pTNM stage (T3 *versus* T1/T2)	4.24 (1.90–9.45)	<0.001	4.14 (1.79–9.59)	0.001
AOC4P (high *versus* low)	1.51 (1.03–2.22)	0.037	1.56 (1.04–2.33)	0.032
Multivariate analysis				
Lymph node (positive *versus* negative)	5.08 (2.27–11.41)	<0.001	5.35 (2.31–12.40)	<0.001
pTNM stage (T3 *versus* T1/T2)	6.54 (2.64–16.20)	<0.001	6.43 (2.44–16.97)	<0.001
AOC4P (high *versus* low)	3.74 (1.50–9.29)	0.005	4.50 (1.68–12.06)	0.003

CI, confidence interval; DFS, disease-free survival; HR, hazard ratio; OS, overall survival; TNM, tumor, nodes, metastasis.

expression, while vimentin and MMP9 expression was reduced [Figure 6(a)]. Western blot assays confirmed these changes at the protein level [Figure 6(b)]. Interestingly, immunofluorescence results of cancer tissues showed that tumors with high expression *AOC4P* had relatively low levels of E-cadherin and high levels of vimentin and MMP9 (Figure 7). Therefore, these results suggest that *AOC4P* modulates GC tumorigenesis by regulating EMT.

Discussion

GC is frequently diagnosed as locally advanced in China, leading to the fact that patients in China have a poor estimated 5-year overall survival of 27.4% compared with 73.2% in Korea.[1,16] One of the solutions to improve prognoses of patients with GC is early detection and intervention strategies. Therefore, we have focused on investigating novel diagnostic markers and potential therapeutic targets of GC.[11,17,18]

Recently we identified five differentially expressed lncRNAs between tumor and adjacent normal tissues by lncRNA microarray profiling, including *TINCR, CCAT2, AOC4P, BANCR*, and *LNC00857*.[11] Using these circulating lncRNAs, we established a five-lncRNA panel for early detection of GC. In the present study, we investigated the role of tissular *AOC4P* in GC. We found significant upregulation of *AOC4P* in GC tissues, and that a high expression level of *AOC4P* was correlated with poor survival and

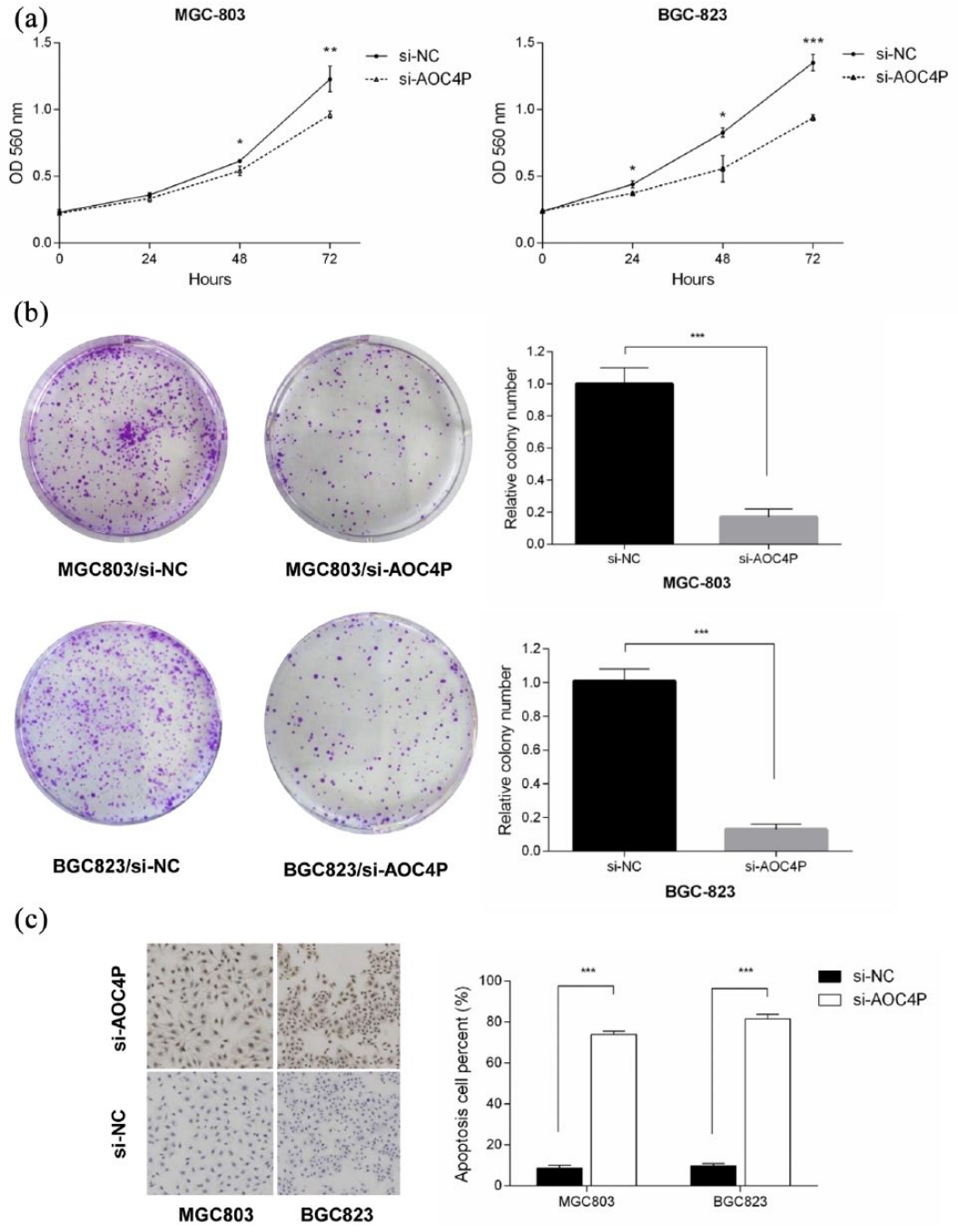

Figure 2. Knockdown of *AOC4P* inhibits proliferation and colony formation and promotes apoptosis *in vitro*. (a) Cell proliferation was measured by MTT assays in MGC-803 and BGC-823 cells. (b) Colony formation assay results. Colonies were photographed and then counted. (c) TUNEL assays to investigate the effect of *AOC4P* on apoptosis of MGC-803 and BGC-823 cells. Results are expressed as the mean ± SD ($n = 3$). *$p < 0.05$, **$p < 0.01$, ***$p < 0.001$.
MTT, 3-(4,5-dimethylthiazol-2-yl)-2,5-diphenyltetrazolium bromide (MTT); SD, standard deviation; TUNEL, terminal deoxynucleotidyl transferase dUTP nick end labeling.

lymphovascular invasion in patients with GC. Functionally, *in vitro* and *in vivo* assays demonstrated that *AOC4P* promoted tumor growth by inducing proliferation, migration, and invasion, and reducing apoptosis. Mechanistically, the oncogenic effect of *AOC4P* in GC might be

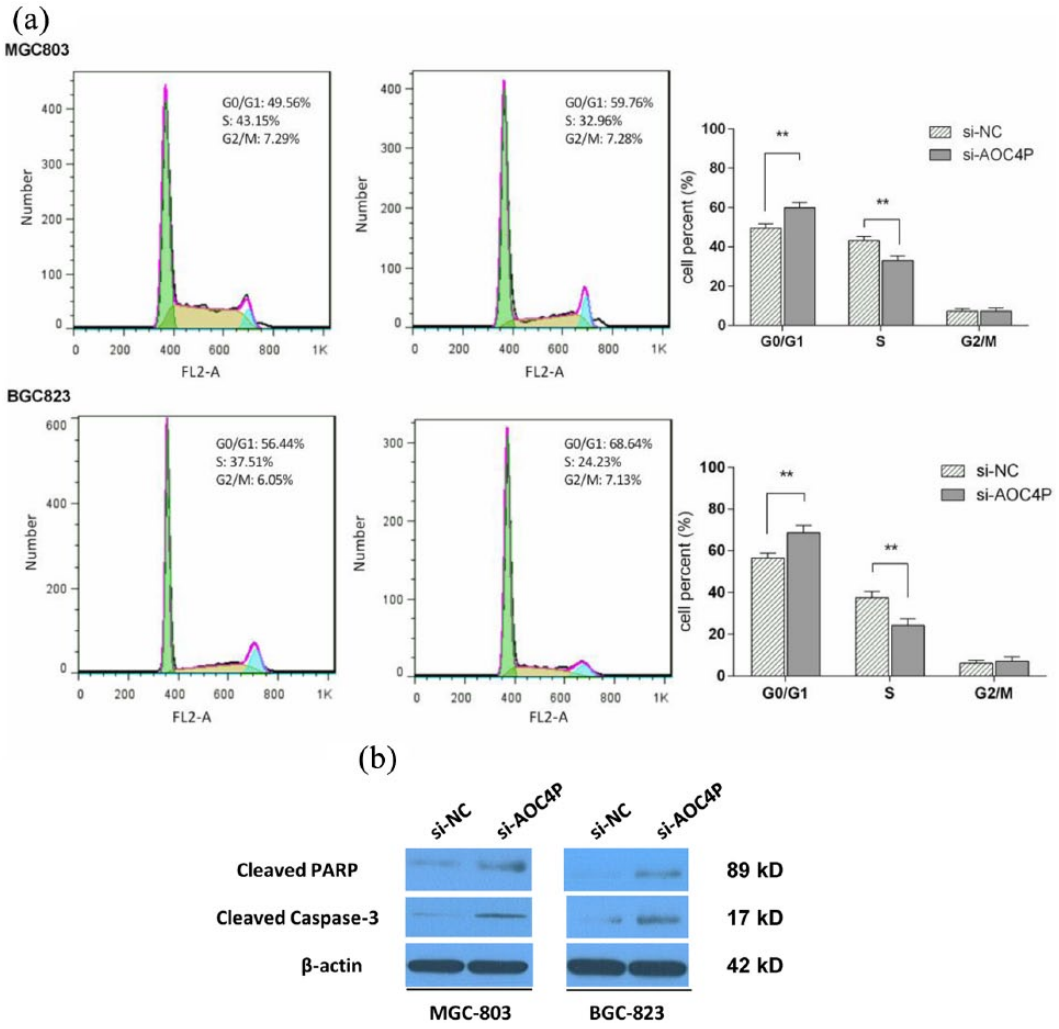

Figure 3. Effect of *AOC4P* on cell cycle and apoptosis-related proteins. (a) Cell cycle analysis in MGC-803 and BGC-823 cells. Knockdown of *AOC4P* induced more number of cells in the G0/G1 phase and reduced the number of cells in the S phase. (b) Apoptosis-related proteins detected by western blotting assay. $^{**}p < 0.01$.

partly attributed to *AOC4P*-mediated EMT. These data are helpful to explain the significance of *AOC4P* upregulation in GC and its correlation with clinicopathological characteristics.

Thus far, the functions of *AOC4P* have only been investigated in colon cancer and hepatocellular carcinoma.[15,19] In colon cancer, *AOC4P* (also termed UPAT) is upregulated in highly tumorigenic colon cancer cells and involved in epigenetic regulation of cancer cells by modulating protein ubiquitination and degradation.[19] Similar to its functions in GC, Taniue and colleagues found that *AOC4P* plays a critical role in tumorigenicity of colon cancer cells.[19] However, in hepatocellular carcinoma, the expression of *AOC4P* was downregulated in 68% of tumor tissues.[15] Our results, together with earlier findings, indicated varied expression of *AOC4P* in different types of carcinomas. A previous study has also reported different expression levels of lncRNA *BANCR* in GC and colon cancer.[20,21] The fact that *AOC4P* is expressed differentially in various carcinomas might be partly explained by its various functions. In this study, we found that inhibition of *AOC4P* increased the expression of E-cadherin, while reducing the expression of vimentin and MMP9. Consistent with these findings, immunofluorescence of tumor specimens confirmed

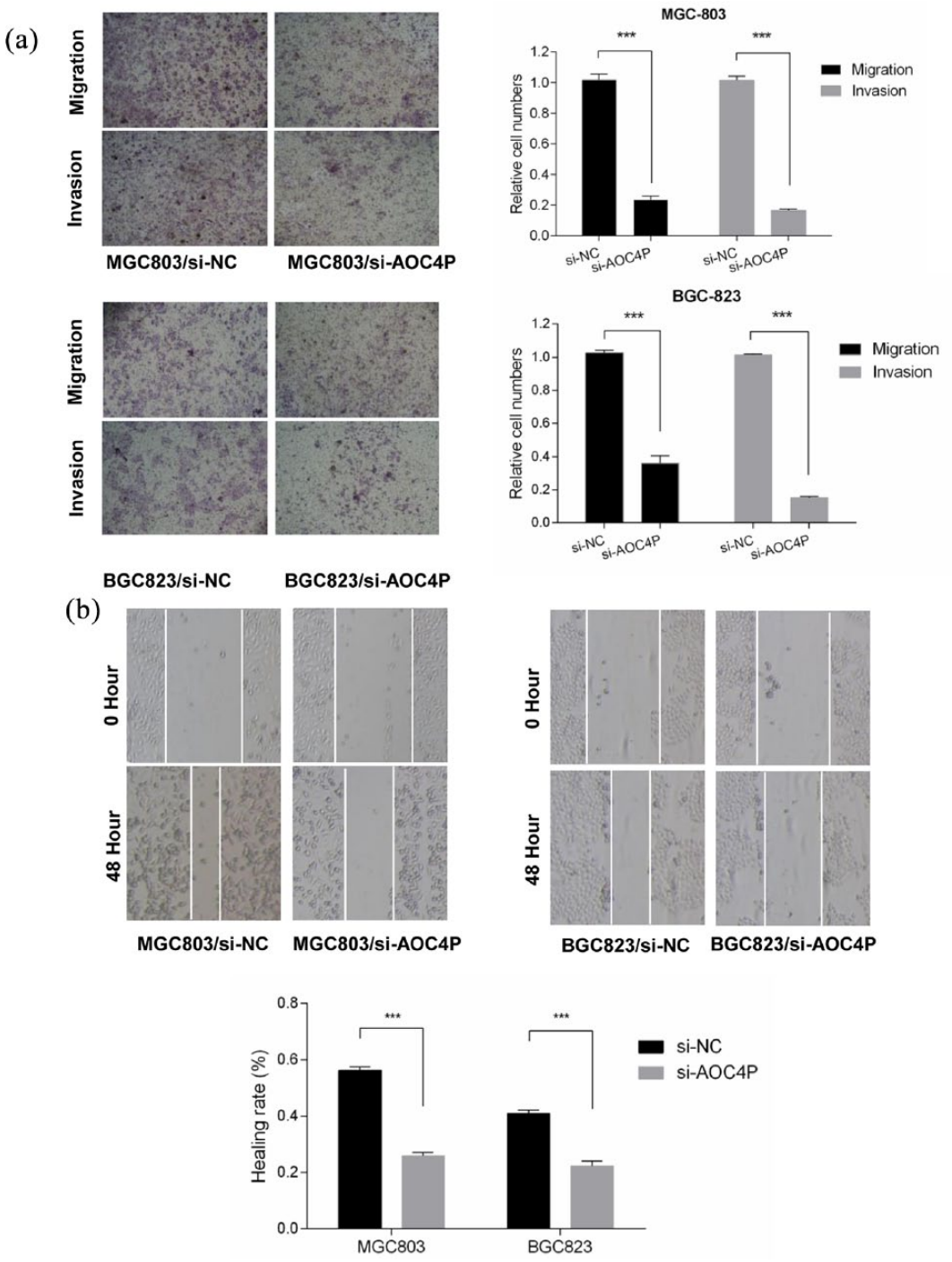

Figure 4. Knockdown of *AOC4P* inhibits migration and invasion *in vitro*. (a) Transwell assays were performed to investigate the effect of *AOC4P* on migration and invasion of MGC-803 and BGC-823 cells. (b) Evaluation of cell motility by wound healing assays in MGC-803 and BGC-823 cells. ***$p < 0.001$.

the correlation of *AOC4P* expression with E-cadherin, vimentin, and MMP9 levels. Therefore, *AOC4P* might exert its oncogenic effect in GC *via* EMT processes.

As a central driver of tumor malignancy, EMT is involved in cancer cell dissemination, drug resistance, subsequent disease recurrence, and acquisition of immunosuppressive capabilities in a

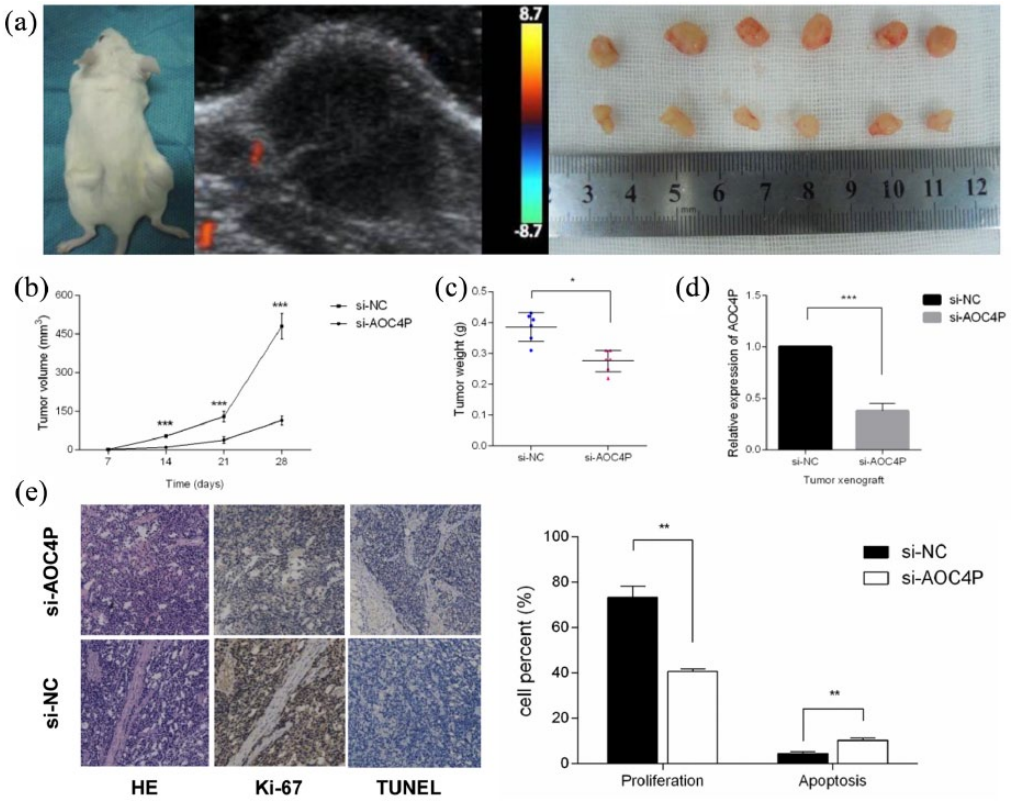

Figure 5. Knockdown of *AOC4P* inhibits tumorigenesis *in vivo*. (a) BGC-823 cells stably transfected with si-*AOC4P* or the empty vector were injected subcutaneously into the left and right flanks of each mouse, respectively ($n = 6$). Representative image of an ultrasound is shown. Upper and lower tumor tissues are si-NC and si-*AOC4P* groups, respectively. (b) Subcutaneous tumor growth curve of the si-*AOC4P* group compared with the si-NC group. (c) Comparison of tumor weights between si-*AOC4P* and si-NC groups. (d) Relative expression levels of *AOC4P* in tumor xenografts. (e) Hematoxylin and eosin staining, Ki-67 expression analysis, and TUNEL assays were performed to evaluate proportions of proliferating and apoptotic cells in tumor xenografts. $*p < 0.05$, $**p < 0.01$, $***p < 0.001$.
si-NC, siRNA negative control; TUNEL, terminal deoxynucleotidyl transferase dUTP nick end labeling.

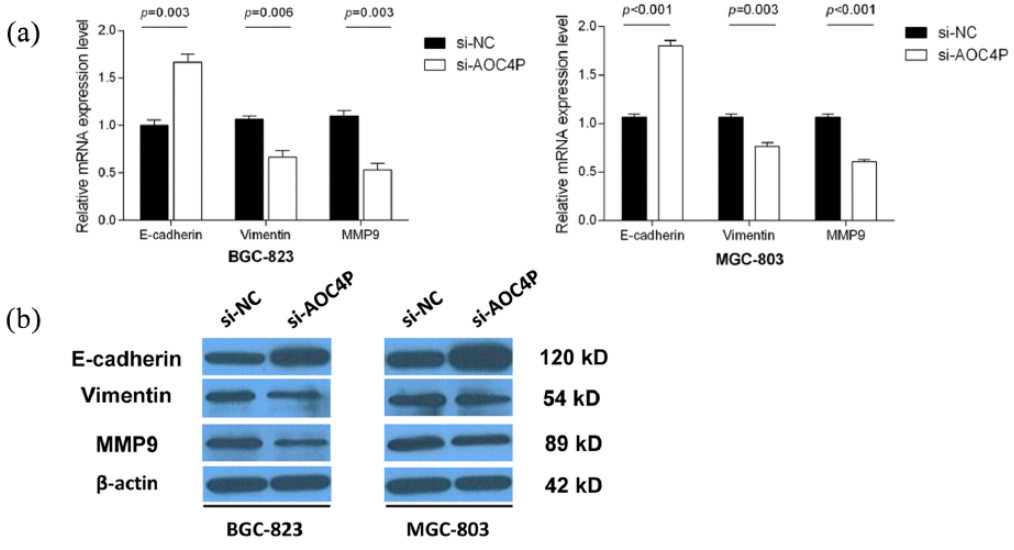

Figure 6. *AOC4P* is involved in EMT processes. (a) Determination of E-cadherin, vimentin, and MMP9 mRNA levels by qRT-PCR following knockdown of *AOC4P* in MGC-803 and BGC-823 cells. (b) Protein expression of E-cadherin, vimentin, and MMP9 analyzed by western blotting after knockdown of *AOC4P* in MGC-803 and BGC-823 cells.
EMT, epithelial–mesenchymal transition; qRT-PCR, quantitative real-time polymerase chain reaction.

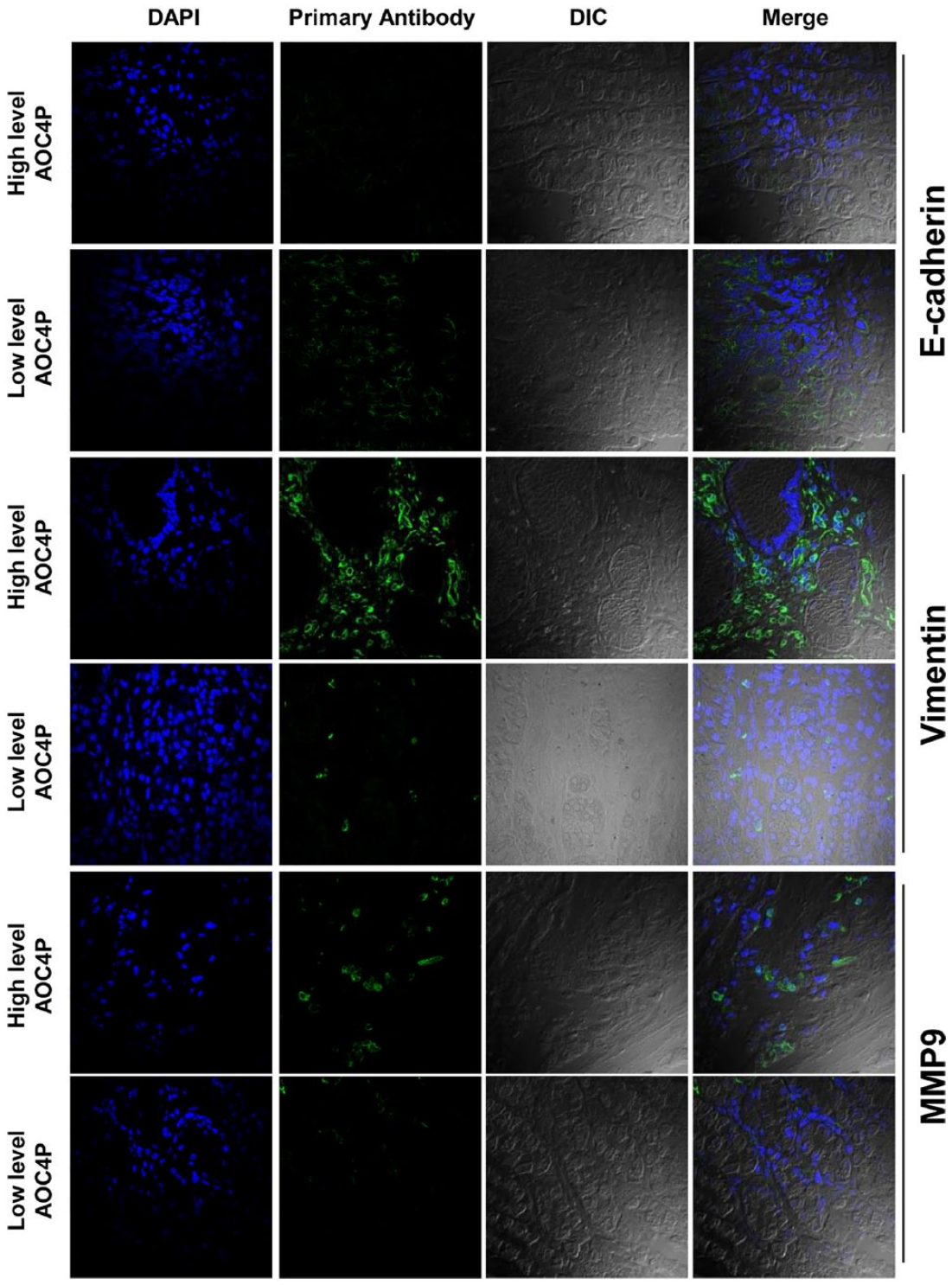

Figure 7. Immunofluorescence of tumor tissues to investigate the association between *AOC4P* expression and E-cadherin, vimentin, and MMP9 levels.

variety of cancers.[22] It has been proposed that essentially all carcinomas develop malignancy-associated characteristics *via* activation of an EMT process in their constituent neoplastic cells.[22] One of the hallmarks of EMT is replacement of E-cadherin by N-cadherin, which results in the

formation of far weaker cell–cell adhesions between adjacent cells. Importantly, a study from the Asian Cancer Research Group has classified GC into four molecular subtypes, among which the EMT type has the worst prognosis, the tendency to occur at an earlier age, and the highest recurrence frequency.[5] Therefore, as a regulator of EMT, *AOC4P* might be a potential therapeutic target for GC treatment.

Our earlier findings demonstrated a correlation between circulating *AOC4P* and tissular *AOC4P*.[11] Circulating lncRNAs in blood are usually incorporated into exosomes, which are small vesicles of endocytic origin that carry a variety of bioactive molecules, including proteins, lipids, RNA, and DNA.[23] Metastasis is a multistep process including invasion of tumor cells into local tissues at a primary tumor site, invasion into blood and lymph vessels, survival in circulation, extravasation from circulation to distant sites, and adaptation and proliferation in the metastatic site. Evidence has shown the involvement of exosomes in all processes of metastasis.[24] Currently, we have only demonstrated that *AOC4P* promoted tumorigenesis and cancer progression intracellularly. Therefore, our future study will focus on how tissular *AOC4P* incorporates into exosomes and is released into circulation, and the role of *AOC4P*-incorporated exosomes in metastatic sites.

Several limitations of present study should be taken into consideration when interpreting the results. First, the prognostic role of *AOC4P* needed to be validated in another independent cohort. Second, we did not unveil the downstream molecules which *AOC4P* regulated, therefore the molecular pathway through which *AOC4P* exerts its function needed a further in-depth investigation.

Conclusion

Taken together, our results revealed a relationship between *AOC4P* and clinicopathological characteristics and demonstrated the prognostic potential of *AOC4P* for GC. We also revealed the involvement of *AOC4P* in proliferation, migration, invasion, and apoptosis of MGC-803 and BGC-823 cells. Our study indicates that *AOC4P* promotes tumorigenesis and progression partly through EMT.

Acknowledgements

Kecheng Zhang, Canrong Lu, Xiaohui Huang, Jianxin Cui are joint authors. Study design and concept: KCZ, CRL, XHH. Data acquisition: YHG, WQL, YL, YS, HXL. Data analysis and interpretation: KCZ, BW, LC. Collection of clinical data and sample disposal: WQL, YL, YS, HXL. Manuscript preparation: KCZ. Manuscript review: BW, LC. All authors read and approved the final manuscript.

Funding

This work was partly funded by the National Nature Science Foundation of China (No. 81672319, 81773135), National Key Research and Development Plan (No. 2016YFC0905302), and Beijing Municipal Science and Technology Plan projects (Z161100000516237, D141100 000414002, Z15110000391547, and Z171100 000417023).

Conflict of interest statement

The authors declare that there is no conflict of interest.

Supplemental material

Supplemental material for this article is available online.

References

1. Zeng H, Zheng R, Guo Y, *et al.* Cancer survival in China, 2003–2005: a population-based study. *Int J Cancer* 2015; 136: 1921–1930.
2. Lee J, Lim DH, Kim S, *et al.* Phase III trial comparing capecitabine plus cisplatin versus capecitabine plus cisplatin with concurrent capecitabine radiotherapy in completely resected gastric cancer with D2 lymph node dissection: the ARTIST trial. *J Clin Oncol* 2012; 30: 268–273.
3. Bang YJ, Kim YW, Yang HK, *et al.* Adjuvant capecitabine and oxaliplatin for gastric cancer after D2 gastrectomy (CLASSIC): a phase 3 open-label, randomised controlled trial. *Lancet* 2012; 379: 315–321.
4. Macdonald JS, Smalley SR, Benedetti J, *et al.* Chemoradiotherapy after surgery compared with surgery alone for adenocarcinoma of the stomach or gastroesophageal junction. *N Engl J Med* 2001; 345: 725–730.
5. Cristescu R, Lee J, Nebozhyn M, *et al.* Molecular analysis of gastric cancer identifies subtypes

associated with distinct clinical outcomes. *Nat Med* 2015; 21: 449–456.

6. Cancer Genome Atlas Research Network. Comprehensive molecular characterization of gastric adenocarcinoma. *Nature* 2014; 513: 202–209.
7. Birney E, Stamatoyannopoulos JA, Dutta A, *et al.* Identification and analysis of functional elements in 1% of the human genome by the ENCODE pilot project. *Nature* 2007; 447: 799–816.
8. Djebali S, Davis CA, Merkel A, *et al.* Landscape of transcription in human cells. *Nature* 2012; 489: 101–108.
9. Fang XY, Pan HF, Leng RX, *et al.* Long noncoding RNAs: novel insights into gastric cancer. *Cancer Lett* 2015; 356: 357–366.
10. Yang Z, Guo X, Li G, et al. Long noncoding RNAs as potential biomarkers in gastric cancer: opportunities and challenges. *Cancer Lett* 2016; 371: 62–70.
11. Zhang K, Shi H, Xi H, *et al.* Genome-wide lncRNA microarray profiling identifies novel circulating lncRNAs for detection of gastric cancer. *Theranostics* 2017; 7: 213–227.
12. Xi HQ, Zhang KC, Li JY, *et al.* RNAi-mediated inhibition of Lgr5 leads to decreased angiogenesis in gastric cancer. *Oncotarget* 2017; 8: 31581–31591.
13. Xi HQ, Wu XS, Wei B, *et al.* Aberrant expression of EphA3 in gastric carcinoma: correlation with tumor angiogenesis and survival. *J Gastroenterol* 2012; 47: 785–794.
14. Gao Y, Cai A, Xi H, *et al.* Ring finger protein 43 associates with gastric cancer progression and attenuates the stemness of gastric cancer stem-like cells via the Wnt-beta/catenin signaling pathway. *Stem Cell Res Ther* 2017; 8: 98.
15. Wang TH, Lin YS, Chen Y, *et al.* Long noncoding RNA AOC4P suppresses hepatocellular carcinoma metastasis by enhancing vimentin degradation and inhibiting epithelial-mesenchymal transition. *Oncotarget* 2015; 6: 23342–23357.
16. Ahn HS, Lee HJ, Yoo MW, *et al.* Changes in clinicopathological features and survival after gastrectomy for gastric cancer over a 20-year period. *Br J Surg* 2011; 98: 255–260.
17. Zhang KC, Xi HQ, Cui JX, *et al.* Hemolysis-free plasma miR-214 as novel biomarker of gastric cancer and is correlated with distant metastasis. *Am J Cancer Res* 2015; 5: 821–829.
18. Shi HZ, Wang YN, Huang XH, *et al.* Serum HER2 as a predictive biomarker for tissue HER2 status and prognosis in patients with gastric cancer. *World J Gastroenterol* 2017; 23: 1836–1842.
19. Taniue K, Kurimoto A, Sugimasa H, *et al.* Long noncoding RNA UPAT promotes colon tumorigenesis by inhibiting degradation of UHRF1. *Proc Natl Acad Sci USA* 2016; 113: 1273–1278.
20. Li L, Zhang L, Zhang Y, *et al.* Increased expression of LncRNA BANCR is associated with clinical progression and poor prognosis in gastric cancer. *Biomed Pharmacother* 2015; 72: 109–112.
21. Shi Y, Liu Y, Wang J, *et al.* Downregulated long noncoding RNA BANCR promotes the proliferation of colorectal cancer cells via downregulation of p21 expression. *PLoS One* 2015; 10: e0122679.
22. Ye X and Weinberg RA. Epithelial-mesenchymal plasticity: a central regulator of cancer progression. *Trends Cell Biol* 2015; 25: 675–686.
23. Lobb RJ, Lima LG and Moller A. Exosomes: key mediators of metastasis and pre-metastatic niche formation. *Semin Cell Dev Biol* 2017; 67: 3–10.
24. Becker A, Thakur BK, Weiss JM, *et al.* Extracellular vesicles in cancer: cell-to-cell mediators of metastasis. *Cancer Cell* 2016; 30: 836–848.